Published in final edited form as:
Chemistry. 2014 September 8; 20(37): 11636–11639. doi:10.1002/chem.201403604.

High-Resolution 3D Proton MRI of Hyperpolarized Gas Enabled by Parahydrogen and Rh/TiO_2 Heterogeneous Catalyst

Dr. Kirill V. Kovtunov[a], **Danila A. Barskiy**[a], **Aaron M. Coffey**[b], **Dr. Milton L. Truong**[b], **Oleg G. Salnikov**[a], **Alexander K. Khudorozhkov**[c], **Elizaveta A. Inozemtseva**[c], **Dr. Igor P. Prosvirin**[c], **Prof. Valery I. Bukhtiyarov**[c], **Dr. Kevin W. Waddell**[b], **Dr. Eduard Y. Chekmenev**[b], and **Prof. Igor V. Koptyug**[a]

Kirill V. Kovtunov: kovtunov@tomo.nsc.ru; Eduard Y. Chekmenev: eduard.chekmenev@vanderbilt.edu

[a]Laboratory of Magnetic Resonance Microimaging, International Tomography Center, SB RAS, 3A Institutskaya St., Novosibirsk 630090 (Russia) and Novosibirsk State University, 2 Pirogova St., Novosibirsk 630090 (Russia)

[b]Institute of Imaging Science, Department of Radiology, Department of Biomedical Engineering, Department of Physics and Astronomy, and Department of Biochemistry, Nashville, Tennessee, 37232-2310 (USA)

[c]Boreskov Institute of Catalysis SB RAS, 5 Acad. Lavrentiev Pr., Novosibirsk 630090 (Russia)

Abstract

Several supported metal catalysts were synthesized, characterized, and tested in heterogeneous hydrogenation of propene with parahydrogen to maximize nuclear spin hyperpolarization of propane gas using parahydrogen induced polarization (PHIP). The Rh/TiO_2 catalyst with a metal particle size of 1.6 nm was found to be the most active and effective in the pairwise hydrogen addition and robust, demonstrating reproducible results with multiple hydrogenation experiments and stability for ≥1.5 years. 3D ^1H magnetic resonance imaging (MRI) of 1 % hyperpolarized flowing gas with microscale spatial resolution (625 × 625 × 625 μm^3) and large imaging matrix (128 × 128 × 32) was demonstrated by using a preclinical 4.7 T scanner and 17.4 s imaging scan time.

Keywords

heterogeneous catalysis; hyperpolarized gas; magnetic resonance imaging; parahydrogen; supported catalysts

Despite the impressive diagnostic power of conventional magnetic resonance imaging (MRI) and computed tomography (CT), there is a fundamental challenge in imaging void spaces such as lungs owing to very low tissue density. As a result, diseases such as chronic obstructive pulmonary disease (COPD) do not have an imaging modality capable of early

Correspondence to: Kirill V. Kovtunov, kovtunov@tomo.nsc.ru; Eduard Y. Chekmenev, eduard.chekmenev@vanderbilt.edu.

Supporting information for this article is available on the WWW under http://dx.doi.org/10.1002/chem.201403604.

disease detection and of monitoring response to treatment during disease onset, when treatments are the most effective. In contrast, molecular imaging of cancer by using ^{18}F-fluorodeoxyglucose (FDG) and other molecular imaging biomarkers revolutionized cancer-patient care for many types of cancer by identifying the treatments that work. In magnetic resonance, hyperpolarization techniques increase nuclear spin polarization by 4–6 orders of magnitude,[1] enabling the use of exogenous hyperpolarized (HP) contrast agents.[2] To date, HP ^{13}C-pyruvate[3] and HP ^{129}Xe have been successfully used in preclinical and clinical imaging of cancer[3] and COPD,[4] respectively. These contrast agents are administered intravenously or by inhalation, respectively, and they enable molecular imaging of biological processes by using HP MRI.[2, 4–5] However, the production of HP ^{13}C contrast agents[6] by dynamic nuclear polarization (DNP)[1a] and HP ^{129}Xe by spin exchange optical pumping (SEOP)[7] requires complex (and costly) hyperpolarization equipment.[6, 8] In addition, MRI with ^{13}C, ^{129}Xe and other hetero-nuclei requires additional radio-frequency (rf) channels and rf probes, which are not standard equipment in commercially available preclinical and clinical MRI scanners.[3]

Therefore, the development of hyperpolarized molecular imaging gas probes with proton detection is highly desired from the perspective of MRI signal read-out. Parahydrogen-induced[9] polarization (PHIP)[10] is ideally suited for this task of HP agent production, because it is relatively simple, high-throughput, and provides molecular contrast agents that can be used for proton MRI detection.

Motivated by the above technical and biomedical challenges, the heterogeneous catalysis work presented here is focused on the development of highly polarized propane gas with the degree of hyperpolarization suitable for high-resolution MRI applications.

PHIP hyperpolarization is based on pairwise parahydrogen addition to an unsaturated substrate, where the symmetry of the singlet state of the nuclear spins of parahydrogen is broken in the final product.[9] PHIP can be based on both homogeneous[11] and heterogeneous[12] catalytic hydrogenations to produce a HP product. However, homogeneous PHIP hydrogenation poses the problem of catalyst separation, which is the main obstacle for its potential biomedical use.[13] Metal (e.g., Rh^I) complexes dissolved in organic solvents can be also used for producing catalyst-free HP fluids by bubbling parahydrogen and substrate gas mixtures through the solution of the homogeneous catalyst,[14] but the volatility of the solvent may be a problem for potential biomedical use. Furthermore, these complexes are prone to oxidation,[15] which can degrade their catalytic activity and HP contrast agent production. Therefore, the most promising candidates for biomedical MRI applications are heterogeneous catalysts that are used in a hydrogenation of the PHIP precursor with parahydrogen in the flowing gas. There are two demonstrated approaches for preparation of such heterogeneous catalysts: (i) metal complexes (already known as effective homogeneous catalysts) immobilized on a solid support,[16] and (ii) metal nanoparticles deposited on a solid support.[12a] Immobilized metal complexes can be unstable under reactive conditions. They can undergo irreversible reduction during highly exothermal hydrogenation processes, especially during gas-phase hydrogenation,[17] and can leach into solution in liquid-phase processes. Supported metal catalysts can be more practical as they can sustain high temperatures, which is convenient from the perspective of

robust use (no complex cooling engineering) and taking advantage of high reaction temperature to increase HP product yields. Additionally, these catalysts may have long shelf-lives (for example, the catalysts used in this work did not lose their catalytic activity after their storage for 1.5 years at normal conditions). To date, only 2D imaging of hyperpolarized gases produced by heterogeneous hydrogenation with parahydrogen has been reported.[18] Here, 3D hyperpolarized gas-phase proton MRI with microscale resolution is reported for the first time based on the use of supported metal catalysts.

Based on our previous results demonstrating that metals supported on titanium oxide (TiO_2) generally exhibit higher levels of PHIP effects compared with other oxide supports, a number of metal catalysts supported on TiO_2 were prepared and characterized (see the Supporting Information). Pd/TiO_2, Pt/TiO_2, and Rh/TiO_2 catalysts with different sizes of metal nanoparticles were tested in the heterogeneous gas-phase hydrogenation of propene. The ALTADENA[19] procedure was utilized, where the hydrogenation reaction is carried out in the Earth's magnetic field and the reaction products are then adiabatically transferred to the NMR spectrometer for detection at 9.4 T (Figure 1 a).

All three catalysts studied were very active in the heterogeneous hydrogenation of propene to propane (Figure 1 b) and, importantly, produced strongly polarized PHIP signals (Figure 1 c) as detected by high-resolution NMR spectroscopy. The catalytic activity of the Rh/TiO_2 catalyst for pairwise hydrogen addition was higher than that for the Pd/TiO_2 and Pt/TiO_2 catalysts with similar metal-particle sizes (Figure 1 d). Four Rh/TiO_2 catalysts with different metal-particle sizes were tested, demonstrating that the nanoparticle size clearly influences the magnitude of PHIP hyperpolarization as seen in Figure S3 (see the Supporting Information). The maximum PHIP signal at 9.4 T was observed with 1.6 nm particles (Figure S3). This catalyst yielded HP propane (flowing gas) with significant signal enhancement compared with the thermally polarized propane (gas flow stopped), Figure 1 c. Therefore, this catalyst was selected for further MRI studies in a 4.7 T preclinical MRI scanner.

Two letter-shaped phantoms were used for flowing HP propane gas MRI experiments: "VU" (standing for Vanderbilt University, Figure 2) and "NSU" (standing for Novosibirsk State University, Figure S4 in the Supporting Information). The phantoms were constructed of Tygon™ tubing (3/32 in. ID × 3/16 in. OD), wrapped around cardboard to construct the proper letter shapes and to provide the phantoms with more depth to invoke better spatial dimensionality in the resulting images. For each hyperpolarized imaging experiment, propene was mixed with parahydrogen in 1:2 molar ratio, which, after the reaction, gave a mixture of hyperpolarized propane and residual unreacted parahydrogen (≈ 1:1 ratio), Figure 1 a. HP propane was actively pumped into the letter phantom cells and released through the outlet without any backpressure or additional flow restriction. A continuous flow rate (15 mL s^{-1}) of the HP propane/residual parahydrogen mix was maintained until the image acquisition was completed. 3D gradient echo images of the phantoms with HP propane gas at flowing conditions were recorded for both letter-shaped phantoms. A representative perspective of 3D MRI image of HP propane with spatial resolution of 0.625 × 0.625 × 0.625 mm^3 is shown in Figure 2 a, and a corresponding 3D MRI image of thermally polarized water with identical imaging parameters except for the rf excitation

pulse angle is shown in Figure 2 b (see the Supporting Information for additional images as well as full 3D rendering movies). Both images were acquired over a very large field of view ($80 \times 80 \times 20$ mm^3) with a large imaging matrix of $128 \times 128 \times 32$ in approximately 17 s, which can be potentially reduced to subsecond speed by using compressed sensing.[20] Despite significant improvement in spatial resolution of < ½ μL per voxel and the addition of the third dimension, the total scan time for the 3D gas MRI was approximately 30-times shorter than the scan time of 2D MRI of PHIP polarized gas demonstrated previously.[18a] This improvement is largely endowed by the relatively large proton hyperpolarization of HP propane gas. Note the imaging artifacts in Figure 2 a, seen as image blurring of flowing HP propane. These artifacts (not present in water reference image) are related to the image encoding on the time scale of a few ms while the gas is flowing rapidly, with the most pronounced signal loss in areas corresponding to the highest gas velocity along *x* axis.

A comparison of HP propane and reference water image shown in Figure 2 indicates that the signal-to-noise ratio (SNR) for water sample was approximately three-times higher than the SNR for the same phantom filled with HP propane. The estimated percentage of pairwise hydrogen addition route was about 1.3 % (see the Supporting Information), which is similar to previously published results.[21] Therefore, even 1.3 % hyperpolarized flowing propane can yield similar quality (as compared to corresponding images of pure water) images at 4.7 T, although future improvements in % *P* of HP propane can potentially increase the signal by up to 2 orders of magnitude. Combined with the lower spin-polarization of water in clinically relevant magnetic fields of 1.5 and 3.0 T, HP propane gas can potentially overshadow the signal from background water protons. Furthermore, high-sensitivity HP MRI in low magnetic fields (<0.1 T) potentially exceeding the sensitivity of high-field detection[22] can offer an alternative water background suppression (scaling linearly with magnetic field strength) well below the signal of HP propane even with the hyperpolarization level demonstrated here.

Although the actual % *P* of HP propane was only about 1.3 %, it should be noted that each propane molecule carries two HP protons, effectively doubling the magnetization pay-load. Furthermore, protons have a significantly higher (3.6–4.0 fold) gyromagnetic ratio than ^{129}Xe and ^{13}C, making 1.3 % polarized propane comparable to approximately 10 % HP ^{129}Xe or ^{13}C. However, we note that, fundamentally, HP propane MRI sensitivity can exceed that of HP ^{129}Xe and ^{13}C if the propane proton hyperpolarization level can be further increased.

To conclude, 3D ^{1}H MRI of HP gas with microscale spatial resolution was demonstrated, enabled by supported metal catalysts. The Rh/TiO_2 catalyst was most efficient among the catalysts tested and yielded 1.3 % proton hyperpolarization (see the Supporting Information). Heterogeneously produced HP propane in combination with 3D MRI may enable a number of applications ranging from imaging of porous media to human lung imaging without requiring isotopic enrichment of hyperpolarized contrast media and by using a relatively simple hyperpolarization setup and conventional (i.e., proton) MRI hardware. Short- and long-term catalyst stability, allowing for preparation of a catalyst-free, nontoxic asphyxiant propane gas, can potentially enable robust preclinical and clinical 3D molecular imaging at subsecond scan times.

Experimental Section

High-resolution NMR spectroscopy was performed by using a Bruker 9.4 T spectrometer for the experiments shown in Figure 1 and Figure S3. Other spectroscopic (see the Supporting Information) and imaging experiments were performed on a Varian 4.7 T animal imaging system using the VNMRJ version 3.3 software suite. The experiments were conducted with a custom-built 38 mm ID two-channel RF coil, with the ^{1}H channel tuned to 200.25 MHz and the other rf channel terminated. All MRI experiments used the shim gradient values obtained from shimming on a 10 mL sample of deionized water in a plastic conical container, resulting in a half-height line width of 3 Hz. Varian's version of a 3D gradient echo (ge3D) was used with a total acquisition time of 17.4 s and a spectrum width (SW) of 40 kHz. The rf excitation pulse had a Gaussian shape with 500 μs width (15° tipping angle for HP propane and 2° for water). Repetition time (TR) was 4.2 ms, and echo time (TE) was 2.1 ms. Imaging resolution was 0.625 × 0.625 × 0.625 mm^3 with imaging matrix 128 × 128 × 32. No compressed sensing or image acceleration was employed. All MRI experiments were conducted by using one of two letter-shaped phantoms, "VU" (Figure 2) and "NSU" (Figure S4). A continuous flow rate (~15 mL s^{-1}) of HP propane/parahydrogen mix was maintained for the duration of imaging acquisition. For the imaging of water, the letter phantoms were completely filled with water, with the inlet and outlet plugged. The PHIP reaction setup depicted in Figure 1 a utilized an Arduino Uno microcontroller board (arduino.cc) connected to a previously used microcontroller driven manifold.[1b] Briefly, the valves depicted as ⊗ were solenoid valves (Peter Paul Electronics, Inc. model number EH22J9DCCM6 24/DC) driven by the microcontroller, and connected using PTFE tubing (1/8 in. OD/1/16 in. ID). The mixing chamber was the 56 mL PHIP reactor used previously,[1b] filled automatically with 2.8 atm of propene (Sigma–Aldrich #295663) and 5.7 atm of >90 % ultrahigh purity (99.999 % +) parahydrogen gas[23] (8.5 atm total pressure). The reactor shown in Figure 1 a was a section of copper tubing (approximately 4 in. long, 1/8 in. OD) connected to the main PTFE line by using push-to-connect connectors. The oven was a heating tape wrapped around temperature-stabilized (ca. 100 °C) copper tubing.

Supplementary Material

Refer to Web version on PubMed Central for supplementary material.

Acknowledgments

This work was supported by the RAS (5.1.1), RFBR (14-03-00374-a, 14-03-31239-mol-a, 12-03-00403-a), SB RAS (57, 60, 61, 122), MK-4391.2013.3. We thank for funding support NIH ICMIC 5P50 CA128323-03, R21 GM107947 5R00 CA134749-03, 3R00A134749-02S1, DoD CDMRP Breast Cancer Program Era of Hope Award W81XWH-12-1-0159/BC112431.

References

1. a) Ardenkjaer-Larsen JH, Fridlund B, Gram A, Hansson G, Hansson L, Lerche MH, Servin R, Thaning M, Golman K. Proc Natl Acad Sci USA. 2003; 100:10158–10163. [PubMed: 12930897] b) Waddell KW, Coffey AM, Chekmenev EY. J Am Chem Soc. 2011; 133:97–101. [PubMed: 21141960]

2. Kurhanewicz J, Vigneron DB, Brindle K, Chekmenev EY, Comment A, Cunningham CH, DeBerardinis RJ, Green GG, Leach MO, Rajan SS, Rizi RR, Ross BD, Warren WS, Malloy CR. Neoplasia. 2011; 13:81–97. [PubMed: 21403835]

3. Nelson SJ, Kurhanewicz J, Vigneron DB, Larson PEZ, Harzstark AL, Ferrone M, van Criekinge M, Chang JW, Bok R, Park I, Reed G, Carvajal L, Small EJ, Munster P, Weinberg VK, Ardenkjaer-Larsen JH, Chen AP, Hurd RE, Odegardstuen LI, Robb FJ, Tropp J, Murray JA. Sci Transl Med. 2013; 5:198ra108.

4. Mugler JP, Altes TA. J Magn Reson Imaging. 2013; 37:313–331. [PubMed: 23355432]

5. Goodson BM. J Magn Reson. 2002; 155:157–216. [PubMed: 12036331]

6. Ardenkjaer-Larsen JH, Leach AM, Clarke N, Urbahn J, Anderson D, Skloss TW. NMR Biomed. 2011; 24:927–932. [PubMed: 21416540]

7. Walker TG, Happer W. Rev Mod Phys. 1997; 69:629–642.

8. a) Ruset IC, Ketel S, Hersman FW. Phys Rev Lett. 2006; 96:053002. [PubMed: 16486926] b) Nikolaou P, Coffey AM, Walkup LL, Gust BM, Whiting N, Newton H, Barcus S, Muradyan I, Dabaghyan M, Moroz GD, Rosen M, Patz S, Barlow MJ, Chekmenev EY, Goodson BM. Proc Natl Acad Sci USA. 2013; 110:14150–14155. [PubMed: 23946420] c) Nikolaou P, Coffey AM, Walkup LL, Gust B, LaPierre C, Koehnemann E, Barlow MJ, Rosen MS, Goodson BM, Chekmenev EY. J Am Chem Soc. 2014; 136:1636–1642. [PubMed: 24400919]

9. Bowers CR, Weitekamp DP. Phys Rev Lett. 1986; 57:2645–2648. [PubMed: 10033824]

10. Eisenschmid TC, Kirss RU, Deutsch PP, Hommeltoft SI, Eisenberg R, Bargon J, Lawler RG, Balch AL. J Am Chem Soc. 1987; 109:8089–8091.

11. Duckett SB, Mewis RE. Acc Chem Res. 2012; 45:1247–1257. [PubMed: 22452702]

12. a) Kovtunov KV, Beck IE, Bukhtiyarov VI, Koptyug IV. Angew Chem. 2008; 120:1514–1517.Angew Chem Int Ed. 2008; 47:1492–1495.b) Balu AM, Duckett SB, Luque R. Dalton Trans. 2009:5074–5076. [PubMed: 19562165] c) Kovtunov KV, Zhivonitko VV, Skovpin IV, Barskiy DA, Koptyug IV. Top Curr Chem. 2012; 338:123–180. [PubMed: 23097028]

13. Golman K, Axelsson O, Johannesson H, Mansson S, Olofsson C, Petersson JS. Magn Reson Med. 2001; 46:1–5. [PubMed: 11443703]

14. Kovtunov KV, Zhivonitko VV, Skovpin IV, Barskiy DA, Salnikov OG, Koptyug IV. J Phys Chem C. 2013; 117:22887–22893.

15. Shchepin RV, Coffey AM, Waddell KW, Chekmenev EY. J Phys Chem Lett. 2012; 3:3281–3285. [PubMed: 23227297]

16. Koptyug IV, Kovtunov KV, Burt SR, Anwar MS, Hilty C, Han SI, Pines A, Sagdeev RZ. J Am Chem Soc. 2007; 129:5580–5586. [PubMed: 17408268]

17. Skovpin IV, Zhivonitko VV, Koptyug IV. Appl Magn Reson. 2011; 41:393–410.

18. a) Bouchard LS, Kovtunov KV, Burt SR, Anwar MS, Koptyug IV, Sagdeev RZ, Pines A. Angew Chem. 2007; 119:4142–4146.Angew Chem Int Ed. 2007; 46:4064–4068.b) Bouchard LS, Burt SR, Anwar MS, Kovtunov KV, Koptyug IV, Pines A. Science. 2008; 319:442–445. [PubMed: 18218891] c) Telkki VV, Zhivonitko VV, Ahola S, Kovtunov KV, Jokisaari J, Koptyug IV. Angew Chem. 2010; 122:8541–8544.Angew Chem Int Ed. 2010; 49:8363–8366.d) Zhivonitko VV, Telkki VV, Koptyug IV. Angew Chem. 2012; 124:8178–8182.Angew Chem Int Ed. 2012; 51:8054–8058.

19. Pravica MG, Weitekamp DP. Chem Phys Lett. 1988; 145:255–258.

20. Sarracanie M, Armstrong BD, Stockmann J, Rosen MS. Magn Reson Med. 2014; 71:735–745.

21. Kovtunov, KV.; Koptyug, IV. Magnetic Resonance Microscopy. Codd, SL.; Seymour, JD., editors. Wiley-VCH; Weinheim: 2009. p. 99-115.

22. Coffey AM, Truong ML, Chekmenev EY. J Magn Reson. 2013; 237:169–174. [PubMed: 24239701]

23. Feng B, Coffey AM, Colon RD, Chekmenev EY, Waddell KW. J Magn Reson. 2012; 214:258–262. [PubMed: 22188975]

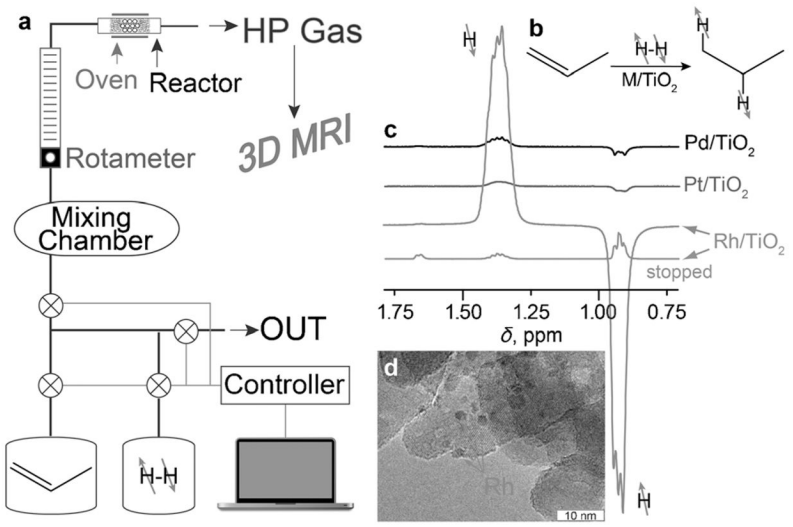

Figure 1.

a) Experimental setup diagram of propane hyperpolarization by PHIP with subsequent 3D MR imaging of letter-shaped phantoms shown in Figure 2. b) Molecular diagram of propene hydrogenation by parahydrogen over M/TiO_2 yielding hyperpolarized propane. c) ^1H NMR (9.4 T) spectra acquired with continuous flow of reaction products after propene hydrogenation with parahydrogen over different TiO_2-supported metal catalysts in Earth's magnetic field with subsequent adiabatic transfer to the magnetic field of the NMR spectrometer (ALTADENA conditions). d) TEM image of the representative Rh/TiO_2 catalyst; arrows indicate the presence of deposited Rh nanoparticles.

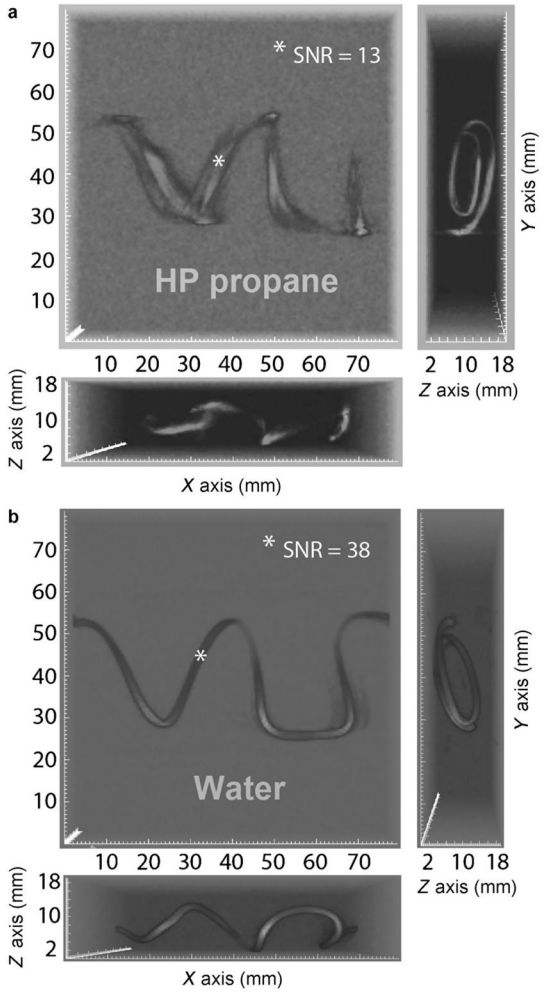

Figure 2.

3D gradient echo (GRE) ^{1}H MRI of flowing HP propane (a) and water reference (b) in "VU"-shaped phantom with three projections shown for each image. Both sets of 3D images have voxel size of 625 × 625 × 625 μm^3 and total imaging time of 17.4 s with TR =4.2 ms, TE =2.1 ms. The field of view (FOV) was 80 × 80 × 20 mm^3 with imaging matrix 128 × 128 × 32. A movie showing the full 3D rendering is available in the Supporting Information.